An Investigation of Fluorine-Hydrogen Main-Tank-Injection Pressurization

E. C. CADY*
McDonnell Douglas Astronautics Company, Santa Monica, Calif.

A comprehensive program was performed to design and test F_2 injectors for main tank injection (MTI) of a space vehicle LH_2 tank. A series of 131 tests in small glass Dewars was performed to define the limits of hypergolicity and study reaction product freezing. A series of 21 large-scale injector tests was performed in a 105-gallon LH_2 tank to demonstrate MTI feasibility and determine pressurization efficiency of three injector configurations. The tests were performed with tank pressures from 30 to 170 psig, and ullage fractions from 8 to 97% for multiple prepressurization and expulsion cycles. The ullage injector exhibited reliable ignition and efficient pressurization through ullage heating. The submerged injectors showed less efficient pressurization and experienced occasional injectant freezing and detonation. The data were approximately correlated to simple pressurization models, and the feasibility and controllability of the MTI technique was demonstrated.

Nomenclature

P_u	=	ullage pressure, psi
p	=	tank pressure rise rate, psi/sec
Q_R	=	heat of reaction, Btu/lb F_2
V_u	=	ullage volume, ft^3 or percent
$\dot{w}_{F_2}$, $\dot{w}_{LH_2}$	=	fluorine and liquid H_2 flow rates, lbm/sec
γ	=	ratio of specific heats
ρ_{LH_2}	=	LH_2 density, lbm/ft^3

Introduction

MAIN tank injection (MTI) is a technique for rocket-vehicle propellant-tank pressurization in which a hypergolic reactant is injected into a propellant tank and the resultant reaction heat release is used to pressurize the tank. Much work has been done with MTI as applied to hypergolic storable propellants.[1] Little work has been done with the hypergolic cryogenic propellants fluorine and hydrogen. The objective of the program described in this paper was to determine, analytically and experimentally, the feasibility, limitations, and operating characteristics of a propellant-tank pressurization system that uses the injection of fluorine into a liquid hydrogen (LH_2) tank to generate pressurizing gas by hydrogen vaporization. The program was conducted in two phases: 1) laboratory tests and 2) large-scale feasibility tests with LH_2 expulsion.

In the laboratory work, the physical variables included injector location (ullage-space injection and submerged injection); F_2 phase (ambient gas, liquid, and saturated vapor), temperature (140 to 520°R) and pressure (65 to 195 psia); and H_2 condition (saturated at 25 to 55 psia). Chemical variables included propellant contaminants and catalytic effects. The tests were performed in small (5 in. diam by 10 in.) glass Dewars. Pressure and temperature measurements and Fastax motion pictures (at 4000 frames/sec) were used to record each test. Expulsion of the LH_2 from the tank was not performed.

Three injection concepts were tested: simple ullage-space injection (US), simple submerged injection (SS), and aspirated submerged injection (SA). "Aspirated," as used here, means that the injected fluorine is used to jet-pump hydrogen into a combustion zone that is separate from the pumping region.

The results of this initial effort led to the following conclusions:

1) Fluorine and hydrogen are generally hypergolic under the conditions that are present when MTI is used to pressurize a liquid hydrogen (LH_2) tank. These propellants normally ignite reliably and have a smooth pressure rise; however, in the simple ullage injection mode (US), it was found that the addition of about 1% (volume) of oxygen (O_2) to the injectant fluorine caused reaction inhibition (Fig. 1). The US injector was a simple tube situated on the tank centerline. It was found that US injection effectively heats the ullage gases, gives maximum pressure rise per weight of injectant and, for the final engine burn of a mission, leaves the LH_2 tank full of hot GH_2, which results in minimum residual propellant weight. The specific pressure rise (psi/lb F_2) was used because the fluorine was slug-injected in 50–100 msec. The reaction inhibition was followed by injectant fluorine freezing in the liquid hydrogen. This frozen fluorine occasionally detonated, especially when cold gas or liquid fluorine injectant was used (Fig. 1).

2) An increased injectant total enthalpy was required to overcome the oxygen-induced inhibition and enable ignition prior to injectant freezing (Fig. 2—the shaded region indicates a band between ignition and nonignition). Ignition was considered to have occurred if a flame was observed—regardless of the strength of the reaction. The injection rate, together with the enthalpy level (or warmth) of the injectant, was important in assuring ignition.

3) In the submerged modes, reliable ignition occurred, even with up to 1.5% O_2 added to the F_2. However, the reaction products (HF) tended to freeze and plug the injector. When a helium preinjection purge was used to alleviate the problem of HF freezing, reaction inhibition again occurred. This inhibition also led to fluorine freezing and occasional detonation.

The submerged injection techniques tended to provide tank pressurization by vaporizing hydrogen, which was a fundamental requirement of the program. However, the SS mode appeared to have two disadvantages when compared to the SA mode: 1) the injectant burns at an uncontrollable mixture ratio that produces indeterminate ullage heating levels and unpredictable pressurization rates, and 2) subsurface burning creates large bubbles that may interfere

Presented as Paper 69-528 at the AIAA 5th Propulsion Joint Specialist Conference, U.S. Air Force Academy, Colo., June 9–13, 1969; submitted June 24, 1969; revision received August 12, 1969. This research was sponsored by NASA Lewis Research Center under Contract NAS 3-7963.

* Senior Engineer, Western Division. Member AIAA.

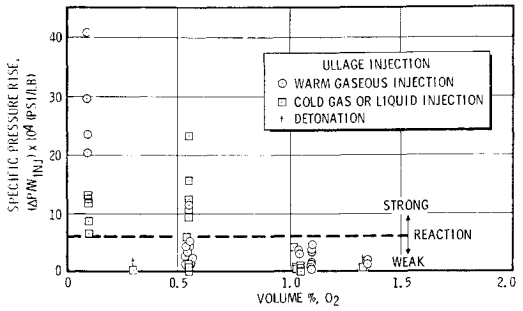

Fig. 1 Effect of O_2 contaminant in injectant on specific pressure rise.

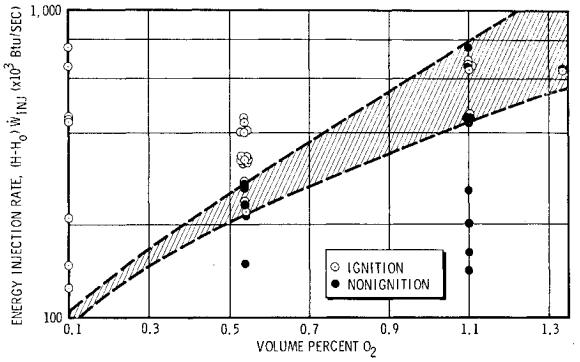

Fig. 2 Effect of O_2 contaminant in injectant on minimum ignition energy.

with normal propellant draining, may severely disturb (slosh) the propellant, and may cause an undesirable transfer of large quantities of heat to the bulk liquid.

The success of the small-scale SA tests indicated that a large-scale SA injector could probably be designed that would aspirate and pump enough LH_2 to provide fuel-rich operation and thus ensure effective vaporization and pressurization. To this end, the fluid dynamics of the SA injector were analyzed to provide basic design data for the large-scale injector.

Previous analyses of aspirators or jet pumps in the literature were unsuitable, because they consider only gas-pumping-gas in a different configuration.[2] An approximate analytical model was developed, therefore, to predict the performance of a gas-pumping-liquid aspirator. Based on this analysis, the large-scale SA injector was designed and fabricated.

Large-Scale Test Apparatus

The injector test apparatus and facility are shown schematically in Fig. 3. There were two basic loops: 1) the LH_2 fill, drain, and vent system and 2) the GF_2 supply and injection systems; the only contact of the two loops was at the injector valve. LH_2 was supplied through a 1-in. vacuum-jacketed fill line to the test tank. The test tank was evacuated through the fill line and through a calcium-hydroxide scrubber that was situated upstream of the H_2 vacuum pump to remove any HF that might have remained in the tank after a test. The LH_2 was drained through a 1-in. vacuum-jacketed line to the drain valve (H6), through the flow orifice, and out the vent stack. The test tank was vented through a 2-in. insulated line to the vent valve (H7) and then through a 2-in. uninsulated line to the vent stack.

The GF_2 control loop supplied fluorine from a standard supply cylinder through the prevalve (F9). The cylinder pressure was monitored by the gage ($GF1$). The injection system downstream of the prevalve was evacuated and F_2-scrubbed through the vacuum valve (F10) and another calcium hydroxide scrubber. The injection system was purged with nitrogen (or helium) through (F13).

The point of contact of the two loops was the injector valve (F14). This valve was a solenoid-actuated, pneumatically (helium) operated valve with a copper-to-stainless-steel seat that was compatible with both liquid and gaseous fluorine.

The test tank was a stainless-steel, vacuum-jacketed, superinsulated LH_2 Dewar, 24-in. i.d. by 60 in. deep. The inner vessel was built to ASME code specifications for a working pressure of 200 psig. A false bottom was used to allow evaluation of the effect of draining on the submerged injector performance. A bottom penetration was provided (for injection) through the vacuum jacket. Except for this small (0.375 in.) bottom penetration, all penetrations were through the test tank cover, which was made from a stainless steel, 150-lb, ASA blind flange. These penetrations included fill, drain, vent, and pressurization lines; light and camera ports, thermocouple and other sensor lead penetrations; and a rupture disc. The light and camera ports were made of 3-in.-diam 0.75-in.-thick polished pyrex.

Because of potential damage from the F_2-H_2 flame and possible corrosive attack by HF and F_2, expensive high-response instrumentation was not used in the tank. Rather, temperatures were measured with shielded thermocouples of 36-gage copper-constantan wire with the reference junction contained in an LN_2 bath. The thermocouples had a response time of about 500 msec. This slow response time was permissible for most of the temperatures that were measured. The pressures were measured with ordinary bridge-type stainless-steel diaphragm transducers.

General Testing Results

US Injector Tests

Eleven US tests were made (tests 4–14 in Table 1) and were, generally, characterized by rapid pressure rise, ullage heating, and pressure collapse following pressurization. In these tests, the fluorine flow rate could be readily varied, with no injectant freezing problem at low flow (as in the submerged tests discussed later). In fact, an injector burning problem occurred. The initial US injectors used in tests 4–6 were constructed from 304 stainless-steel and burned off at the point where they passed through the test tank lid in all three tests. A hot spot apparently formed where the injector tube passed through the lid because of insufficient cooling capacity in that area. The failure mechanism seemed to be that molten metal fluoride was formed, and this molten fluoride

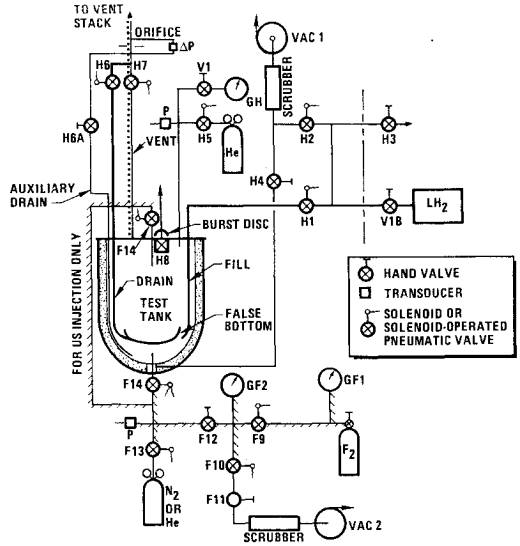

Fig. 3 MTI injector test facility schematic.

Table 1 Injector test summary

Test No.	Mode	V_u,[a] %	$p_{T_i}/\bar{p}_T$, psig	$\bar{w}_{LH_2}$, lb/sec	$\bar{w}_{F_2} \times 10^4$, lb/sec	$\bar{T}_u$, °R	$w_{F_2} \times 10^3$, lb
1	SS	8.2	21/25	1.23	75	67	124
2	SA	8.3	34/14	0.78	104	184	271
		53.2	...	NE[b]	0	...	
3	SA	8.3	110/20	1.3	22	109	65
4	US	8.3	53/30	1.55	26	301	78
		86.0	15/14	1.06		528	
5	US	8.3	173/129	3.77	96	407	282
6	US	8.3	61/114	3.47	98	302	380
		94.3	18/18	1.15		356	
7	US	8.3	81/33	1.68	21	181	130
		62.5	8/10	U[b]		...	
8	US	8.3	32/24	1.38	16	328	76
		48.6	29/24	1.40		242	
		75.8	21/14	1.05		172	
9	US	8.3	31/28	1.48	17	131	65
		37.8	28/23	1.32		256	
		65.2	27/17	1.10		244	
10	US	8.3	110/97	3.51	72	256	141
11	US	8.3	103/97	3.50	68	266	195
		64.5	89/78	3.00		320	
12	US	8.3	150/92	3.40	55	253	250
		51.2	142/95	3.45		320	
13	US	8.3	52/50	2.45	43	284	206
		92.2	28/25	1.70		268	
14	US	8.3	67/66	2.60	43	289	250
		53.9	35/38	1.90		312	
		87.8	35/31	1.65		341	
		97.0	26/22	1.25		365	
15	SA	8.3	28/23	1.49	40	162	65
		62.9	...	NE	0	...	
16	SA	8.3	39/48	1.80	104	250	466
		65.2	10/18	1.14		126	
17	SA	8.3	34/42	1.85	87	175	391
		70.5	37/48	1.95		209	
18	SS	8.3	18/48	1.43	120	132	434
19	SS	8.3	112/73	2.50	92	74	759
		43.8	109/107	3.00		140	
		87.0	111/90	2.80		258	
20	SS	8.3	50/34	1.56	35	94	87
		30.1	...	NE	0	...	
21	SS	8.3	53/46	1.73	68	88	380
		39.4	31/36	1.50		...	
		64.4	36/47	1.75		131	

[a] Ullage volume; tests 1, 3, 5, 10, and 18 were complete expulsion; all others, partial expulsion, with 2, 3, or 4 expulsions performed, beginning with the V_u's shown.
[b] NE = no expulsion; U = unknown.

flowed down the injector, causing it to plug and burn off. Often, the bottom 3 in. or so of the injector was found in the tank bottom.

Injectors made of a high-temperature nickel alloy (A-286) were used in tests 7 and 8; these burned off exactly as did the 304 stainless-steel injectors. An aluminum injector was used for test 9 and showed only mild damage at the tip and some discoloration where it passed through the lid. The aluminum injector was used again for test 10A, and showed rather severe melting at the tip (but no fluoride formation) after it had been used for 63.5 sec and 0.282 lb of fluorine had passed through it. Since it was then apparent that high thermal conductivity materials were beneficial, a copper injector was used next. This injector showed no damage after five runs (tests 10–14); it had then been used for a total of 200 sec and 1.042 lb of fluorine flow.

SA Injector Tests

It was originally hoped that a pyrex SA injector could be used for all tests, so that the flame pattern could be observed with high-speed motion pictures; however, in test 1 (Table 1), this injector shattered immediately upon injection (and ignition), probably because of the thermal shock of ignition. What followed was essentially SS mode injection that, together with additional SS test data, is discussed later. Tank pressurization and expulsion was accomplished without further incident. In test 2, a 316 stainless-steel injector was used with a high fluorine flow rate. It was inferred from the results that the high fluorine pressure blew the flame into the ullage, instead of allowing it to stay in the flame holder (expansion) region of the injector. This flame burned off one of the flame-deflector supports, warped the injector nozzle with heat, and corroded the test tank lid to form metal fluoride deposits. However, the injector apparently aspirated (pumped LH_2) and pressurization and expulsion were successfully accomplished.

For test 3, $\dot{w}_{F_2}$ and pressure were reduced, so that the flame would remain in the expansion region of the injector and not jump into the ullage. Fluorine was injected and apparently froze in the injector. The shock of normal injector valve closure apparently initiated a rapid reaction in the frozen fluorine (which may have been a detonation) that gave a tank pressure rise of over 80 psi in 50 msec, and shattered the metal injector. Pressurization continued to 110 psig, and expulsion followed without further problems.

Because of these SA injector problems, the injector analysis was modified to reflect the actual injector configuration and a series of simulated propellant tests (using GN_2 and water) were performed using the SA injector. The results of this injector performance mapping indicated that the SA injector would run extremely oxidizer rich and would not be capable of pumping excess LH_2 (run fuel rich), keep the injector cool, and perform its desired function of vaporizing hydrogen in a predictable manner for tank pressurization. Further, the oxidizer-rich ratio could be expected to burn indeterminately throughout the length of the injector and in the ullage. The burning would be extremely hot, give no injector heating protection, and lead predictably to injector burning.

To verify the oxidizer-rich performance of the SA injector, a series of large-scale tests using GF_2 and LH_2 were performed. In test 15, an aluminum injector and the false bottom were used. Again, as in test 3, the fluorine froze in the injector and subsequently exploded; this destroyed the injector tube (but did not damage the top part of the injector). No further injection and expulsion was possible. Following this test, it was concluded that the use of the false bottom was imposing an unnecessarily severe environmental constraint on the submerged injector, because it required the fluorine to flow through an additional 8 in. of LH_2-temperature tubing. The false bottom was removed, and the injector tube shortened, so that the tube just penetrated the tank. In addition, to further assure elimination of the injectant freezing problem (and thus properly evaluate the SA injector performance) the injector tube was made of copper, was heated during the test (to approximately 160°F), and was purged with helium between drains. These supplemental measures were eliminated one by one in tests 16–18, and there was no further freezing problem.

It was clear from the test data and from examination of the injector that the SA injector, as predicted, was not pumping sufficient LH_2 and was operating extremely oxidizer-rich; this caused high flame temperatures. There was extensive injector damage despite the fact that the injector was buried in LH_2. It appeared pointless, therefore, to continue with additional SA tests, because it was believed that SS injection could provide equivalent pressurization efficiency without the risk of injector burning and potential tank damage.

SS Injector Tests

Tests 18–21 were made with a short copper SS injector, with no injector heating, and no helium postpurge between drains. Except for test 20, there was no further injectant freezing problem. During test 20, the fluorine metering valve (F12 in Fig. 3) burned, with the result that $\dot{w}_F$ was very low, and the injectant froze in the injector. There were two explosions during injection, but there was no injector damage; however, the injector was plugged with frozen HF and neither further injection nor the planned second drain was possible. The SS mode runs gave pressurization characteristics quite similar to those of the SA mode.

Injectant Freezing and HF Problems

For the submerged injection tests, injectant freezing was a persistent possibility. Tests 3, 15, and 20 failed to achieve all test objectives because of injectant freezing. To define testing parameters that would ensure that injectant freezing did not occur, the heat transfer to the injector was analyzed. The data correlated remarkably well with the standard Dittus-Boelter forced-convection heat-transfer correlation.

When HF froze in the LH_2, apparently most of it was drained along with the LH_2 during the testing, as evidenced by the severe corrosion of the drain line, drain valve, and flow control orifices; however, a considerable quantity of HF was left on the tank walls after the tests. It is believed that the drain line corrosion was caused by the aqueous HF solution that was formed by water vapor that condensed in the line after testing. It is apparent that HF can be a problem in a flight system, particularly if there are noncompatible materials downstream of the tank, or if the HF becomes deposited in a place where it can warm up or come in contact with water.

Wall Heating

Excessive tank wall heating was anticipated as a potential problem during the US tests with high ullage heating. During the tests, some wall heating was found, but it was not significant from a structural standpoint. As shown in Table 1, the average ullage temperature, $\bar{T}_u$, reached a maximum of 528°R, but the measured wall temperature never exceeded 110°R. Although the test tank was not flightweight (0.188-in. walls), no wall-heating problems are anticipated for a vehicle application of the US mode, because of the demonstrated insulating and heat-sink potential of the hydrogen ullage vapor.

Pressurization Results

Tank Prepressurization

A simple model is useful for describing rapid prepressurization by pure heat addition to the tank. The assumption of pure heat addition is appropriate for F_2-H_2 MTI, because small quantities of injectant give large quantities of heat, and the reaction products condense, giving essentially no pressurization benefit. The model assumes that all of the pure heat addition is used to uniformly raise the temperature (and thus the pressure) of the initial ullage gas. Tank pressure rise rate (for perfect gas in the ullage) as a function of injection rate and ullage volume is

$$\dot{p}/\dot{w}_{F_2} = (\gamma - 1)Q_R/V_u \qquad (1)$$

For a nearly full LH_2 tank, the ullage may not be a perfect gas, but may consist of saturated vapor. Equation (1) may also be used for saturated vapor, if the value of γ is chosen properly based on the properties of saturated hydrogen. The model does not account specifically for losses of heat through heat transfer to the bulk liquid or the tank walls. Such losses reflect as a decrease in pressure rise-rate compared to the ideal models.

The analytical results were computed for an initial tank pressure of 20 psia and are plotted with the parameters $\bar{p}_T/\bar{w}_{F_2}$ vs V_u in Fig. 4 (line A-A). The prepressurization data for the small- and large-scale tests are also shown in Fig. 4 with the small-scale test data in the upper left. The small-scale data shown do not include all tests, but only those that were performed under similar test conditions as the large-scale tests, namely, tests using ambient-temperature GF_2 injectant, and tests that showed vigorous reaction with no inhibition caused by oxygen content, or use of a preinjection helium purge.

The data scatter may be caused by the fact that V_u in the small-scale tests varied indeterminately by perhaps 20%,

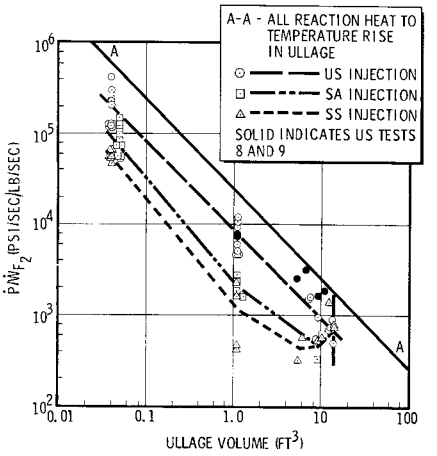

Fig. 4 Prepressurization correlation.

but all data were plotted at the estimated mean ullage volume of 0.04 ft^3.

The large-scale data also show some scatter at $V_u = 1.1$ ft^3; this is attributable to errors in V_u determination (except for the SS data scatter, which may be attributed also to the basic pressurization indeterminacy of the mode). The pressure rise-rate data were based on the longest available injection times for each run, to reduce the effect of transient surges. Only data taken during prepressurization (at constant tank volume) were included.

The US test data follow the analytic trend well, except that tests 8 and 9 (solid points) show an upward trend in pressurization rate in the vicinity of $V_u = 7$ ft^3. With the data from these runs ignored, the averages of the US data at each V_u fall on the straight dashed line shown. The anomalous behavior of tests 8 and 9 and the reasons for the increased pressurization in these runs is discussed in detail later.

The SA test data also correlate well from the small-scale ullage volume up to $V_u = 6$ ft^3. Then the pressurization curve rises sharply until it is similar to the US mode at $V_u = 13$ ft^3 (empty tank). This is because the SA (and the SS) injection mode is severely penalized by heat losses to the liquid hydrogen. As the tank empties, the losses are reduced, and all modes tend to pressurize at the same rate. This effect is clearly shown when the tank is full of liquid ($V_u = 1.1$ ft^3). The heat losses are large enough to push the pressurization rate averages down to only 8% of the predicted value.

For the SS tests, the correlation trend is the same, and for the same reasons, except that the basic pressurization correlation line is lower than for the SA mode. This is because the SA mode (even in the small-scale tests) generally exhibited some ullage space burning, which reduces the propensity for heat-transfer losses to the liquid hydrogen.

Pressurization efficiency (actual $\dot{p}/\dot{w}$ divided by $\dot{p}/\dot{w}$ from Eq. 1) vs amount of ullage is plotted in Fig. 5 for selected anomalous and typical runs. Each of the points shown was for successive prepressurizations during each particular run; thus, only runs that tested with multiple drains are shown. Test 14 is a typical US mode test with high pressure F_2 injection. The pressurization efficiency starts fairly high and remains high until the ullage volume increases to the point where the additional heat-transfer losses (probably to the tank walls) take effect and drive the pressurization efficiency down. The pressurization characteristics of tests 8 and 9 were different from all of the other US runs because the fluorine driving pressure in these runs was very low (<20 psi). This low driving pressure resulted in low fluorine injection velocity, and thus, minimum penetration of the flame into the LH_2. Initially, with the tank full, the penetration (and thus the losses) is similar for all US runs. As the tank empties,

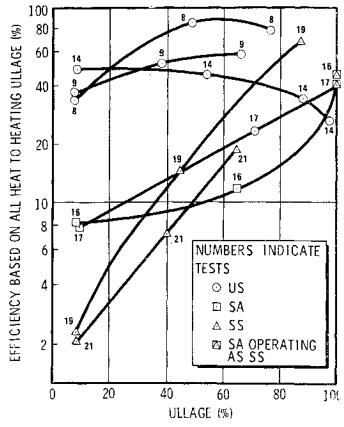

Fig. 5 Prepressurization efficiency.

however, the efficiency of tests 8 and 9 rises, because the low velocity flame does not penetrate the LH_2 and lose heat as it did during the other US runs. Again, as the ullage volume continues to increase, the increased heat losses to the tank walls drives down the efficiency of tests 8 and 9.

As mentioned previously, the SA tests have low efficiency with a full tank because of the long heat-transfer path through the LH_2. As the tank empties the heat losses drop, and the SA efficiency approaches that of the US injector.

The SS test pressurization efficiency is interesting in that it is extremely low (2%) with a full tank, but increases linearly with ullage volume increase (or decrease in liquid level, heat-transfer length) and also approaches the US efficiency with an empty tank.

With large ullage volume (and empty tank), all of the injection modes tend to an efficiency value of about 40% of the pressure rise rate expected based on ullage heating. Thus the ullage heating that occurs from these modes results in efficient pressurization.

Expulsion Pressurization

MTI may also be used for propellant tank expulsion pressurization for vehicle systems with pressure-fed engines (systems with pump-fed engines would probably use hydrogen bled from the engines for tank pressurization during expulsion). For this reason, it is also of interest to compare the relative efficiency of the injection modes when used for propellant expulsion pressurization.

The model for expulsion pressurization assumes that all of the pure heat addition is used to uniformly heat the ullage gas so that the ullage pressure is maintained constant as the ullage volume expands (i.e., the liquid in the tank is removed). The equation derived for perfect gas in the ullage, giving liquid outflow rate as a function of injection rate and ullage pressure is

$$\dot{w}_{LH_2}/\dot{w}_{F_2} = (\gamma - 1)Q_R\rho_{LH_2}/\gamma P_u \qquad (2)$$

Again, for a saturated vapor ullage, Eq. (2) gives accurate results with the correct choice of γ.

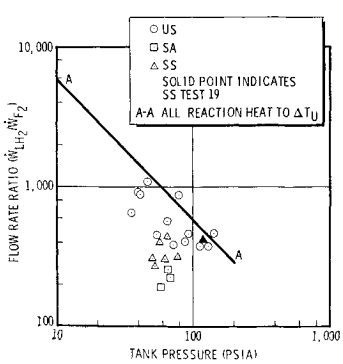

Fig. 6 Expulsion pressurization correlation.

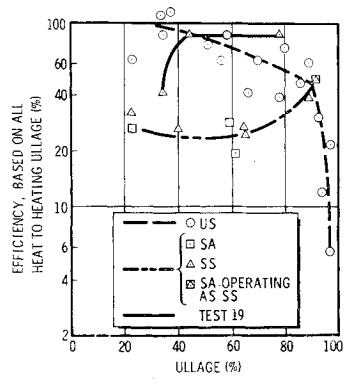

Fig. 7 Expulsion pressurization efficiency.

As in the prepressurization analysis, the expulsion analysis does not account for heat losses, which reflect as a decrease in expulsion efficiency compared to the ideal. The analytical results are plotted, together with the test data, for flow rate ratio ($\dot{w}_{LH_2}/\dot{w}_{F_2}$) vs P_u in Fig. 6 (line A-A).

The calculations for ullage heating (Eq. 2) again assumed a $\gamma = 1.7$. The large-scale test data shown (no expulsion was performed in the small-scale tests) were taken from expulsion data where the tank pressure was essentially constant during both LH_2 draining and fluorine injection. These conditions did not necessarily occur during some tests, and occurred several times on others. The data shown were computed on the basis of the average tank pressure during the selected time span. The average expulsion flow rate was computed on the basis of this average tank pressure. The average fluorine-driving pressure during the selected drain time was used to determine the fluorine-injection rate. Further, the data were computed only for drains with ullage volume less than 90% of tank volume, for reasons that are explained below. As could be expected from the averaging technique, there is some data scatter, but it appears no worse than the scatter for the prepressurization data for which the determining variables were better controlled. The US data clearly follow the trend predicted by the model with the submerged data lower in performance (except for the solid point, which represents an interesting anomalous test which is discussed in detail below).

It was found that amount of ullage volume had a strong influence on the expulsion pressurization efficiency, even though no such volume dependence appeared in the simplified analytical model. This is thought to be the result of ullage-volume-dependent heat-transfer losses that are not accounted for in the analysis. The effect is not surprising because ullage-volume-dependent efficiency losses were observed in the prepressurization data discussed previously. To evaluate this ullage volume effect, the expulsion pressurization efficiency [actual $\dot{w}_{LH_2}/\dot{w}_{F_2}$ divided by the $\dot{w}_{LH_2}/\dot{w}_{F_2}$ from Eq. (2)] at the particular tank pressure, was plotted vs average ullage volume percent (during the selected drain interval) in Fig. 7.

The US data drop off in efficiency with increasing ullage volume (displaying the same trend noted in the prepressurization data) up to an ullage fraction of 90%. At this point, the efficiency drops abruptly, probably because of vapor pull-through, which occurred when the tank was nearly empty.

The submerged tests follow a different trend, with the efficiency remaining relatively constant but lower than the US value, until the tank is nearly empty, when the efficiency rises to match that of the US mode. This trend is similar to that found for the prepressurization efficiency.

Test 19 is shown because the test data are quite different from the other SS (or SA) data. The efficiency during this drain was very high (86%) and similar to the efficiencies shown for US mode injection. The reasons for this anomalous behavior appear to be that this particular submerged run was made for prepressurization and expulsion at high tank-pressure (100 psig) which required high-pressure, high flow

rate, fluorine injection. Long prepressurization times (23 sec) were required to reach 100 psig, and this long, continuous, high-velocity fluorine injection probably created a hole in the LH_2 that reached from the injector to the ullage along the tank centerline. The vapor in this ullage extension was heated by injection in the same way that US mode injection heats the ullage, which gave a high initial pressurization efficiency that is comparable to that of the US mode. Further, at this high tank pressure, the LH_2 outflow rate was quite high, so that the drain from an ullage fraction of 44–78% (shown as the straight solid line) took place in only 6.6 sec. This short time gives little opportunity for heat transfer and could explain the fact that efficiency remained uniform and high. Again, with large ullage volume (and empty tank), all of the injection modes tend to an efficiency value of about 50% of the ullage heating prediction.

Conclusions

Fluorine injection into a liquid hydrogen tank provides efficient tank pressurization by ullage heating, rather than by vaporization of hydrogen. Manual control of the pressure during prepressurization and expulsion has been demonstrated, and the extension to an automatic tank-pressure control system appears straightforward.

The ullage-simple injector mode demonstrated an efficiency of 40–80% for tank prepressurization and propellant expulsion. The submerged aspirated injector did not operate satisfactorily: it could not pump (by aspiration) sufficient hydrogen for vaporization and injector cooling. The injector always operated extremely oxidizer(fluorine)-rich and very hot, which resulted in severe damage to the injector as the tank emptied. The submerged-simple injection mode has pressurization efficiency of about 2% operating into a full tank, because of large heat losses to the liquid. The efficiency improves to as much as 40% as the tank empties. Work is in progress to develop models that include provisions for heat-transfer modes, to permit more confident extrapolation from the existing test data to arbitrary tank sizes and liquid levels.

References

[1] Kenny, R. J. and Friedman, P. A., "Chemical Pressurization of Hypergolic Liquid Propellants," *Journal Spacecraft and Rockets*, Vol. 2, No. 5, Oct. 1965, p. 746–753.

[2] Van Der Lingen, "A Jet Pump Design Theory," *Transactions of the ASME Series D: Journal of Basic Engineering*, Dec. 1960, pp. 947–960.

NOVEMBER 1969 J. SPACECRAFT VOL. 6, NO. 11

Measurement of Solid Rocket Motor Thermally Induced Radial Bond Stresses

W. H. MILLER*

Rocketdyne, A Division of North American Rockwell Corporation, McGregor, Texas

Through-the-case, semiconductor load transducers† were utilized in a prototype solid propellant rocket motor to monitor thermally induced, case-to-liner normal bond stresses. Grain cross-sectional design was cross dogbones; length-to-diameter ratio was 5.5. Six thermal cycles were made between 160° and −65°F. Characteristics of the transducers are discussed briefly, and data for nine longitudinal and circumferential stations are presented. Characteristics of the stress increase/decay with conditioning temperature reduction/rise are described along with the reductions in magnitudes which were measured with each ensuing temperature cycle. Bond stresses predicted analytically are compared with measured data.

Introduction

THE analyst is required to predict stress-strain magnitudes and distributions induced in nonlinear viscoelastic materials when designing case-bonded, solid propellant rocket motor grains. The stress induced in the liner and propellant at the case bond line is of prime interest. Numerical techniques currently used by industry for stress-strain predictions, although most useful, require numerous limiting approximations. These are involved in the selection of the mathematical model, approximating analytically the properties of viscoelastic materials, and the analytical duplication of the load-inducing, motor environmental conditions. Ultimate success of a grain design analysis is measured by the ability of production grains to endure service environments without failure. Thus, it is desirable to measure stress-strain states in full-scale motors and by so doing to obtain guidance and assurance with respect to the assumptions necessary to permit confident analytical assessments of the structural capability of future grain designs.

As one step toward accomplishing this objective, Rocketdyne developed a semiconductor load cell that permits the analyst to experimentally determine normal stresses at the bond line between two rheologically different materials. This instrumentation was first used in tests of 4-in.-diam test vehicles containing case-bonded propellant grains with cylindrical ports.[1] Ensuing tests were made with a prototype structural test motor more representative in size and configuration of a full-scale missile propulsion system.[2] Results from the latter are presented herein. Loads were induced thermally by temperature cycling under development-program-type test conditions.

Presented as Paper 68-510 at the ICRPG/AIAA 3rd Solid Propulsion Conference, Atlantic City, N.J., June 4–6, 1968; submitted October 21, 1968; revision received August 4, 1969. This work was supported by Rocketdyne's Independent Research and Development Program, 1966–1967. Numerous members of the technical staff at Rocketdyne contributed significantly to this program. The author is especially thankful to J. D. Burton for his assistance with data evaluation.

* Member of Technical Staff, Solid Rocket Division. Member AIAA.

† Patent 3,389,598.